PHILOSOPHICAL TRANSACTIONS OF THE ROYAL SOCIETY A MATHEMATICAL, PHYSICAL & ENGINEERING SCIENCES

Strategies and Protocols for Clinical ^{31}P Research in the Heart and Brain [and Discussion]

Paul A. Bottomley, Christopher J. Hardy, P. Mansfield, R. G. Shulman and D. Menon

Phil. Trans. R. Soc. Lond. A 1990 **333**, 531-544
doi: 10.1098/rsta.1990.0181

Strategies and protocols for clinical ^{31}P research in the heart and brain

By Paul A. Bottomley and Christopher J. Hardy

GE Corporate Research and Development Center, PO Box 8, Schenectady, New York 12301, U.S.A.

Although *in vivo* ^{31}P NMR permits unique measurements of the body's stores of high energy phosphate metabolites, their low concentrations place critical limits and demands on spatial resolution, localization techniques, and reproducibility. We argue that optimum reliability and reproducibility of *in vivo* measurements of metabolite ratios and concentrations is best achieved by preselecting the minimal requirements for spatial localization suited to, and varying with, the particular organ and disease type. Strategies for measuring metabolite ratios and concentrations in the human heart and brain are discussed and demonstrated in the context of the expeditious choice of operating parameters, including localized volume size, localization technique, NMR coils, radiofrequency-field uniformity, patient positioning, and corrections for spectral distortion caused by NMR relaxation, to optimize the return of useful metabolic information in practical clinical research exams of about an hour duration.

1. Introduction

What information can a spectroscopy exam provide that is of benefit to patient diagnosis, therapy, or the understanding of disease processes, and which cannot be more easily, safely or cheaply obtained by other means? Upon this question rests the fate of *in vivo* chemical shift nuclear magnetic resonance (NMR) spectroscopy in clinical medicine. Clinical spectroscopy research strategies generally respond by identifying chemical moieties of potential value that are uniquely observable with NMR spectroscopy and then by seeking either to document abnormalities in those moieties in patients or to characterize their response to intervention (Bottomley 1989; Radda *et al.* 1989). For example, *in vivo* phosphorus (^{31}P) NMR spectroscopy is unique in its ability to provide non-invasive access to human high-energy phosphate metabolism. NMR imaging, ultrasound, X-ray, nuclear and positron emission tomography can provide sensitive anatomical pictures or measurements of flow or substrate uptake, but not of adenosine triphosphate (ATP), the body's fundamental energy currency. Disorders involving suspected disturbances in energy metabolism such as ischemic disease, tumours and congenital metabolic abnormalities are therefore major targets for clinical ^{31}P NMR research.

The critical problem for ^{31}P NMR is the millimolar-level phosphate metabolite concentrations which occur *in vivo* and result in ^{31}P NMR signal-to-noise ratios (SNRs) for metabolites some 10^{-5} of those of proton (^{1}H) NMR in tissue water (Bottomley 1989). As the intrinsic SNR of a single ^{1}H NMR free induction decay from tissue water is 20–80 μl^{-1} $Hz^{\frac{1}{2}}$ at 1.5 T using a head or smaller (6 cm) circular surface detection coil

(Edelstein *et al.* 1986), the factor of 10^{-5} can only realistically be accommodated by sacrificing spatial resolution. Thus the finest resolution yet achieved with localized ^{31}P spectroscopy of the human brain or heart is around 10–30 ml (Bottomley *et al.* 1988, 1990*b*; Tropp *et al.* 1988; Coutts *et al.* 1989; Weiner *et al.* 1989). This is inadequate for providing useful anatomical pictures, especially of the heart with wall dimensions of *ca.* 1 cm. An alternative imaging modality is therefore essential for defining the anatomical location of the source of the ^{31}P spectra. Because of the direct relationship between NMR imaging and spectroscopy localization techniques, conventional ^{1}H NMR imaging is an obvious choice for this function (Bottomley 1985), and should form an integral part of clinical spectroscopy research protocols that involve either focal disorders or organs whose morphology varies on a scale comparable with the resolution.

But there are other pitfalls in performing quantitative clinical ^{31}P spectroscopy research even at 10–30 ml resolution. Firstly, such spectra are invariably acquired under conditions of partial saturation with sequence repetition periods (T_R) typically much lower than the metabolite spin-lattice relaxation times (T_1) which can measure up to 6 s (Buchthal *et al.* 1989). It is not feasible to acquire unsaturated 10 ml human brain or heart spectra at $T_R \geqslant 15$ s ($\geqslant 3T_1$) within tolerable patient exam times totalling *ca.* 1 h. This means that metabolite measurements are not comparable unless either they are acquired under identical saturation conditions or they are reliably corrected for saturation. A second problem is that spectra are most often acquired with highly non-uniform transmitter and/or receiver NMR coils (Bottomley *et al.* 1988, 1990*b*; Weiner *et al.* 1989; Tropp *et al.* 1988), which means that additional spatially dependent saturation and/or amplitude corrections are necessary for comparative quantification. Each additional correction increases the probability of error and decreases the reliability of the results (Bottomley *et al.* 1988; Bottomley & Hardy 1989). Thirdly, at 10–30 ml or coarser resolution the problems of tissue heterogeneity, most commonly manifested as spectra containing unknown mixtures of signal contributions for normal and abnormal tissue, remains a most significant problem for the study of focal diseases.

All of these problems are not simultaneously soluble within the nominal hour-long total patient NMR exam. To acquire usable results, disturbing trade-offs must therefore be made usually between resolution and accuracy:

$$(\text{field strength})^{-1} \propto (\text{scan time})^{-\frac{1}{2}} \propto \text{resolved volume} \propto \text{fractional precision (SNR)}.$$

Even increasing the field strength from 1.5 to 4 T for human studies does not dramatically improve matters, except by permitting a $(2.7^2 = 7.1)$-fold increase in the number of ^{31}P NMR measurements that can potentially be made in the same exam time, all else being constant (Hardy *et al.* 1988). Because the trade-offs between spatial resolution and relaxation state, RF field uniformity, and the ^{31}P SNR critically affect the reproducibility and comparability of data, the localization technology should be considered as a variable adjusted to optimize the quality of the desired metabolic information for each clinical research protocol. The maximum localized volume (voxel) size that is reasonably suited to the pathology of interest should be chosen. Here we discuss options applicable to protocols for the brain and heat. A protocol decision tree is depicted in figure 1.

PHILOSOPHICAL TRANSACTIONS OF THE ROYAL SOCIETY A MATHEMATICAL, PHYSICAL & ENGINEERING SCIENCES

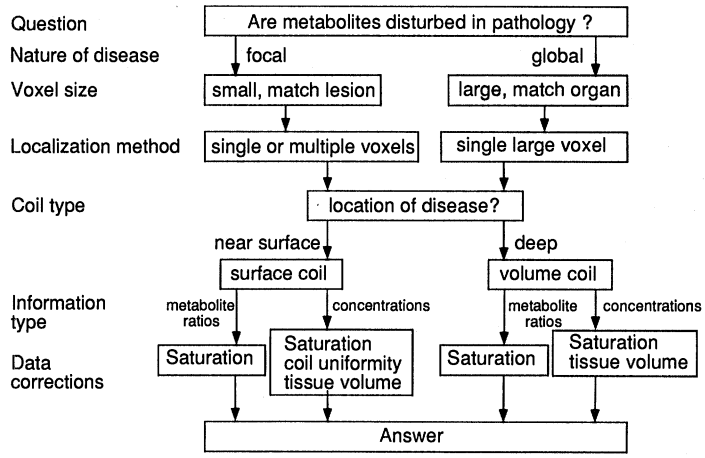

Figure 1. Protocol decisions in clinical ^{31}P research.

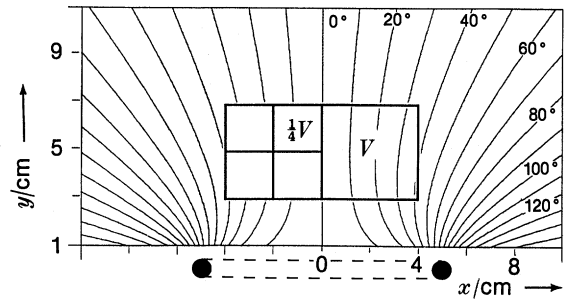

Figure 2. Preselection of a localized volume V or of subvolumes $\frac{1}{4}V$ in the field of view of a 10 cm diameter surface coil located at bottom (solid circles connected by horizontal dashed lines). A two-fold SNR advantage usually results by selecting V as opposed to selection of $\frac{1}{4}V$ sized voxels and subsequent addition of spectra. Contour lines, symmetric about $x = 0$, show the phase of the transverse field of the coil.

2. Preselection of maximum voxel size

As in ^{1}H NMR imaging (Edelstein *et al.* 1986), there is often a significant penalty in the SNR in the localized spectrocopy experiment if the operator chooses to acquire data at a finer spatial resolution than is necessary, and then to subsequently recombine the signals from the multiple voxels that comprise a desired selected volume. This is illustrated in figure 2 for a surface coil spectroscopy experiment. Suppose the localization experiment is adjusted to select a volume V that closely matches that of the desired lesion or region of interest, producing an SNR of S/N. In another experiment, V is resolved into four smaller voxels of volume $\frac{1}{4}V$, for example, using spectroscopic imaging. To create a spectrum from V by using data acquired in the latter experiment, the signals and noises must be added. In all experiments the noise amplitude is the same, independent of voxel size, so the combined r.m.s. noise voltage is $(\Sigma_4 N^2)^{\frac{1}{2}} = 2N$. The signal is proportional to voxel volume so the total signal is $\Sigma_4 \frac{1}{4}S = S$ as before, provided that the spectral resolution and the signal phase is the same in $\frac{1}{4}V$ as in V. The net SNR for a spectrum from V in this experiment is therefore $S/2N$, or only half of that achieved if the data were acquired at a resolution of V in the first place.

This result is independent of the uniformity of both the amplitude of the detection field and the distribution of S in V. However, the amount of SNR that is lost may be reduced or even eliminated if either the main magnetic field or the phase uniformity of the field produced by the detection NMR coil is much worse across V than across $\frac{1}{4}V$, provided that spectra from the $\frac{1}{4}V$ elements can be corrected for phase and chemical shift differences before their combination. For example, figure 1 shows the phase contours for a 10 cm surface coil (Bottomley *et al.* 1990*b*). The phase variation across V is $\beta \approx 40°$ compared with *ca.* 20° across any of the $\frac{1}{4}V$ elements. The signal attenuation factor due to phase cancellation across V assuming a uniform phase variation and uniform excitation field is $\Phi = 2/\beta \sin \frac{1}{2}\beta = 0.98$ (Bottomley *et al.* 1990), against $\Phi = 0.99$ for the $\frac{1}{4}V$ elements. Thus in this case the two-fold SNR penalty for the $\frac{1}{4}V$ experiment remains. In fact, not before β exceeds 200° across V will the disadvantage of the $\frac{1}{4}V$ experiment disappear. This is an unlikely scenario because the region of interest in a surface coil study is usually arranged to fall near the surface coil axis where the phase variation is smallest. On the other hand if the spectral line widths are broadened by the main field inhomogeneity, as opposed to spin–spin relaxation (T_2) processes, and the line widths in $\frac{1}{4}V$ are twice as sharp as those from V as a whole, then the signals from the $\frac{1}{4}V$ elements will be doubled and the disadvantage of the $\frac{1}{4}V$ experiment will vanish. However, in ^{31}P spectra, ATP line widths are around 30 Hz or 1.2 p.p.m. at 1.5 T, which is usually broader than the main field homogeneity over a whole head in a 1 m bore system (Bottomley *et al.* 1984*b*) so this scenario is also usually inapplicable.

In real *in vivo* ^{31}P experiments therefore, there is a major SNR advantage in preselecting the maximum voxel size matched to the tissue region of interest before acquisition. This underscores the need for ^{1}H imaging as a guide and preview to anatomical selection.

3. Choice of NMR coils

NMR coil design has played a prominent role in human spectroscopy localization strategies ever since surface coils alone were used to substantially localize ^{31}P spectra to muscle and brain (Ross *et al.* 1981; Edwards *et al.* 1982; Cady *et al.* 1983; Bottomley *et al.* 1984*b*; Bottomley 1989). We have evolved five radio frequency (RF) coil geometries that are presently in use for heart and brain studies: a short 'stubby' birdcage coil (Bottomley *et al.* 1988) and a long birdcage coil (Bottomley & Hardy 1989) both for excitation and detection of ^{31}P NMR in the head, and three coaxial coplanar distributed-capacitance surface coils for the chest comprising a large square ^{31}P transmit coil, a small circular ^{31}P receiver coil (Bottomley *et al.* 1990*b*), and a small figure-eight shaped ^{1}H receiver coil (Bottomley *et al.* 1989*a*). The geometries are depicted in figure 3. All coils are constructed of 12 mm copper strip and/or 3 mm copper tube conductor and ceramic chip tuning capacitors mounted in plexiglass formers. They are fixed to tune in the magnet with a typical subject present at an impedance of $50 \pm 15\ \Omega$ on resonance: the resonant frequency is tuned by adjusting the capacitors distributed around the coil, the impedance is adjusted with a simple capacitance divider at the cable input (Bottomley *et al.* 1990*b*). Distributing the capacitance effectively eliminates changes in the coil resonant frequency due to varying patient loads, which is a serious problem with the traditional lumped tuning element approach. All coil tuning steps may thus be omitted from the patient study protocol.

Birdcage RF coils were chosen for volume studies of the brain because they offer

PHILOSOPHICAL TRANSACTIONS OF THE ROYAL SOCIETY A MATHEMATICAL, PHYSICAL & ENGINEERING SCIENCES

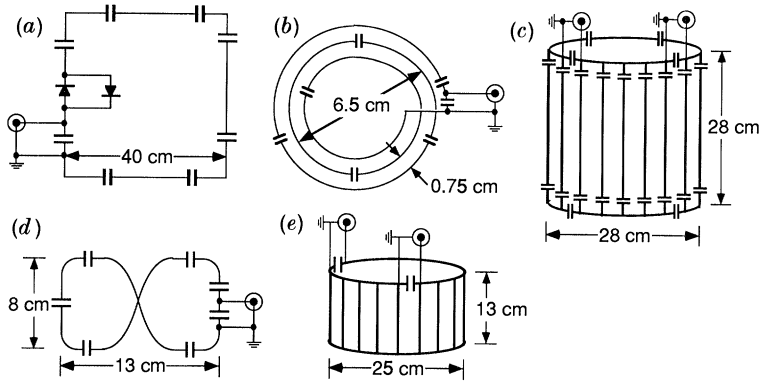

Figure 3. Surface coil (*a*, *b*, *d*) and volume head coil (*c*, *e*) geometries for clinical ^{31}P NMR heart and brain studies. All geometries use distributed tuning capacitors and the tuning and impedance matching are fixed. Receiver coils (*b*–*e*) are connected to preamplifiers by half-wavelength cables. Coils in (*a*, *b*) and (*e*) are coplanar and coaxial. Birdcage coils (*c*, *e*) comprise 16 elements: capacitors on vertical elements in (*e*) are omitted for simplicity. Quadrature inputs are separated by 90° of arc and produce a field rotating in the transverse (horizontal) plane.

superior field uniformity in the azimuthal dimension (Hayes *et al.* 1985). These coils are operated in quadrature with dual inputs separated by 90° and passive mixing circuitry described previously (Bottomley *et al.* 1988), to provide a $\sqrt{2}$-fold SNR advantage over conventional linear operation (Glover *et al.* 1985). The long coil is useful for absolute brain metabolite concentration measurements because the field uniformity across the central plane over the head is better than $\pm 5\%$ (Hayes *et al.* 1985), eliminating troublesome corrections for inhomogeneous partial saturation during excitation and for non-uniform detection (Bottomley & Hardy 1989). The stubby coil provides a 1.5-fold or more improvement in SNR over the long coil, at a considerable cost to field uniformity across the central plane (Bottomley *et al.* 1988). It is useful for acquiring ^{31}P spectra at the highest spatial resolution from multiple voxels, or in spectroscopic imaging studies of the brain. However, the study protocol must incorporate steps that compensate for spatially dependent saturation and detection sensitivity, if results from multiple studies are to be compared. The field profiles for the coils of figure 3 are plotted in figure 4.

Concern about the spatial variation of the excitation field and the consequent inhomogeneous partial saturation also underlies the design of the coil set for heart studies. Thus the 40 cm^2 ^{31}P transmitter coil (figure 3) provides a substantially uniform excitation over the entire range of the sensitive volume of the 6 cm ^{31}P receiver coil (figure 4). To prevent coil coupling from ruining the transmit/receive properties of these coils, the transmitter coil conductor is broken and fitted with crossed-diodes to turn it off during reception, and the receiver coil is fitted with crossed-diodes and a small choke in a resonant circuit across one of the distributed capacitors to turn it off during excitation (Bottomley *et al.* 1990*b*). Finally, the figure-eight shaped coil permits ^{1}H image reception from a similar sensitive volume as the ^{31}P receiver coil, without disturbing the subject. The ^{1}H NMR signal is also used for shimming the main magnetic field homogeneity over the sensitive volume. The advantage of the figure-eight geometry is that although it is coplanar, its field is orthogonal to the other surface coils, resulting in minimal mutual coupling and excellent ^{1}H NMR image/signal reception.

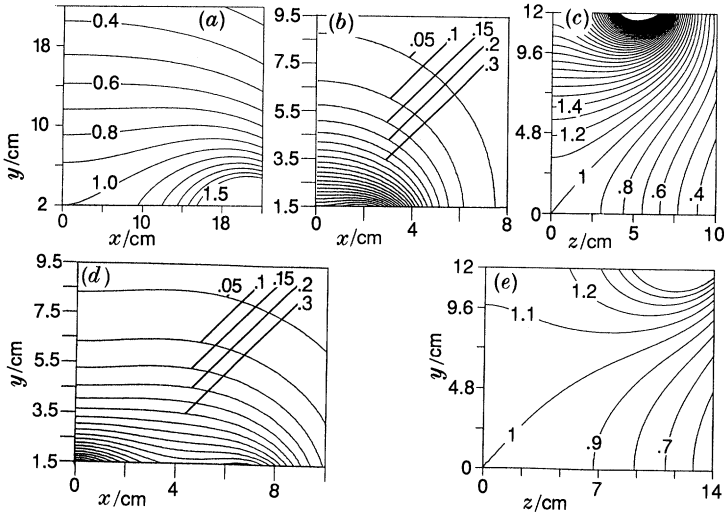

Figure 4. Plots of NMR sensitivity and/or transverse field intensity produced by the 40 cm (*a*), 6.5 cm (*b*), and 8×13 cm (*d*) surface coils, and the 25×13 cm (*c*) and 28×28 cm (*e*) birdcage coils shown in figure 2. Contours are normalized to 1.0 at $x = 0$ (*a*, *b*, *d*) or (*c*, *e*) where (0, 0, 0) is at the coil centre. In (*c*) and (*e*), the *z*-axis coincides with the cylindrical axes of the birdcage coils and the direction of the main field. The figure-eight coil is oriented with long axis parallel to the *x*-axis.

4. Choice of localization techniques

The choice of localization technique should reflect realistic goals of the clinical research study and our golden rule of using the maximum suitable voxel size, or the least possible localization. Spectra from the heart and brain cannot be obtained via surface or volume coil detection alone due to contamination from skeletal muscle, liver or other organs. Human spectroscopy localization methods use either gradients in the RF excitation field, or gradients in the main magnetic field analogous to conventional ^{1}H imaging techniques, as reviewed elsewhere (Aue 1986). We choose the latter class of techniques because of their compatibility with ^{1}H imaging, the versatility of control of the location and size of voxels in all three dimensions afforded by the use of imaging gradients but not current RF gradient techniques, and to avoid problems caused by spatially dependent partial saturation and/or distortions caused by limited excitation bandwidths when long RF encoding pulses are used (Bottomley 1989).

There are two basic localization options with imaging gradients: spatially selective excitation with gradients applied during an amplitude and/or frequency modulated NMR pulse (Bottomley *et al.* 1984*a*; Ordidge *et al.* 1986; Bottomley & Hardy 1987), and spatial encoding where gradient pulses of stepped amplitude are applied after excitation in a scanning sequence (Brown *et al.* 1982). These are depicted in figure 5. Unlike ^{1}H imaging, gradients cannot in general be applied during data acquisition, but the localization procedures can be combined in many different ways with the three orthogonal linear gradients to localize one or more voxels in one to three dimensions (1–3D) as desired.

When spectra from multiple voxels are required, for example, to compare normal and tumour tissue or where the location of an ischemic region is uncertain, 1–3D spatial encoding is the method of choice because the SNR of each voxel after a scan

PHILOSOPHICAL TRANSACTIONS OF THE ROYAL SOCIETY A MATHEMATICAL, PHYSICAL & ENGINEERING SCIENCES

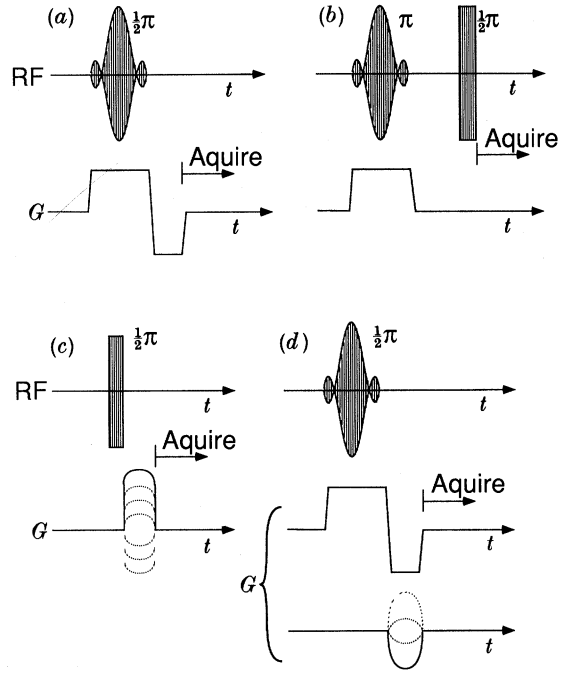

Figure 5. Selective excitation uses a modulated RF excitation pulse in the presence of a pulsed magnetic field gradient G, applied, for example in the x, y, or z directions, to select a plane orthogonal to the gradient direction. It can be performed with a nominally $\frac{1}{2}\pi$ (*a*) or a π (*b*) NMR pulse. Spectra from multiple volumes can be encoded with gradient pulses G applied after a conventional excitation pulse, by scanning the gradient amplitude (*c*). Slice selection and encoding pulses can be combined for gradients in one or more dimensions to achieve full three-dimensional localization (*d*). Sequences in (*a*, *c*, *d*) result in a finite delay before data acquisition.

of duration T is the same as that achieved if the signal from an equivalent voxel were averaged for the same period. Thus to acquire spectra of equivalent SNR from eight adjacent voxels, a single voxel technique would take eight times longer than an eight-step encoding sequence. Although simultaneous multiple voxel acquisition is possible with spatially selective pulses by interleaving excitations during T_R (Bottomley *et al.* 1985), for heart applications this results in the undesirable feature of having spectra acquired at different depths corresponding to different phases of the cardiac cycle. On the other hand, encoding techniques using FT spatial reconstruction (Brown *et al.* 1982; Blackledge *et al.* 1987) can result in contamination of a spectrum in one voxel by 0–25 % or so of the signal in an adjacent voxel due to discrete sampling in the spatial domain, depending on the heterogeneity of the NMR sources relative to the spatial resolution with smaller amounts of contamination resulting when the signal is relatively uniform within voxels (Bottomley *et al.* 1989*b*).

Selective excitation can either be performed with the nominal 90° excitation pulse (Bottomley *et al.* 1984), or with a 180° inversion pulse, preceding excitation (Ordidge *et al.* 1986). The advantage of 90° selective excitation is that only the selected region is excited at any time so the technique is insensitive to motion artefact (Bottomley & Hardy 1987). It is therefore useful for ^{31}P heart studies (Bottomley 1985). Its disadvantage is the delay time, T_d, of several milliseconds after excitation before acquisition can commence, which is required for gradient refocusing (figure 5). This

causes spectral distortion due to missing data points and T_2 decay, which is fast (*ca.* 10 ms) for ATP, raising additional problems for absolute quantification that require correction (Bottomley *et al.* 1988). The advantage of 180° selective inversion is that since it may be followed by a conventional hard (90°) excitation pulse, the acquisition delay and its associated problems are eliminated, permitting more reliable quantification (Bottomley & Hardy 1989). The disadvantage is that at any time, all of the sample is excited by the hard pulse. The selective 180° pulse must be applied and not applied in subsequent applications of the sequence and the resulting signals subtracted to achieve localization (Ordidge *et al.* 1986). Since the signals are large, their difference is highly susceptible to motion (Bottomley & Hardy 1987) so this technique is not recommended for the heart.

5. Orienting the patient and volume-averaged saturation corrections

Cardiac spectroscopy can be performed with the patient oriented prone or supine. A prone orientation with the surface detection coil against and beneath the chest has always been our preference (Bottomley 1985) because it brings the myocardium closest to the coil, thereby resulting in maximum sensitivity. It also minimizes the range of motion of the myocardium due to breathing by fixing the chest location, and it eliminates coil motion compared with a supine orientation with surface coil on top. For studies involving the left ventricle (LV) and apex, the subject is also rotated *ca.* 30° on the left side to orient the anterior wall approximately parallel to the horizontal plane of the surface coil. Figure 6 demonstrates the effect of patient orientation on the depth of the LV from the surface on one normal volunteer. In the supine position the centre of the anterior LV is 57 mm from the surface compared with 30 mm for the prone orientation. This is largely due to some chest compression. The sensitivity plots for the 6.5 cm ^{31}P surface coil show relative sensitivities at 30 mm and 57 mm of about 0.25 and 0.08 on axis. Thus the prone orientation provides a three-fold SNR improvement for cardiac spectroscopy over the supine orientation in this subject. This is a major advantage. We have studied about 100 patients with the prone protocol and have found it reasonably well tolerated for NMR exams lasting 40–75 min when the detection coil is surrounded by foam padding.

To ensure that the myocardial anatomy, location and physiological status are the same at each acquisition period during a ^{31}P scan, it is customary to trigger data acquisitions from a cardiac monitoring transducer such as an ECG lead or an optical peripheral gate. An advantage of the latter is its insensitivity to spurious motions in the magnetic field, compared with ECG leads. This assumes greater importance for ^{31}P studies involving exercise stress testing (Bottomley *et al.* 1989*c*; Conway *et al.* 1988). A direct consequence of cardiac gating is that since typical normal and patient heart rates at rest can vary, in our experience, from 50 to 110 and even higher with exercise, T_R can change by a factor of two or more in any study population, resulting in significant variations in spectral distortion through partial saturation. Since NMR sensitivity limits the ability to acquire fully localized but not fully relaxed ^{31}P NMR spectra, we make the correction with saturation factors, F, derived from unlocalized (surface coil) spectra acquired in every subject at $T_R = 15$ s (unsaturated) and at the T_R, RF transmitter power, and pulse length used for acquiring the localized spectra (Bottomley *et al.* 1989*c*, 1990*b*). This correction assumes that the metabolites in the tissues contributing to the unlocalized spectrum, for example from both

PHILOSOPHICAL TRANSACTIONS OF THE ROYAL SOCIETY A MATHEMATICAL, PHYSICAL & ENGINEERING SCIENCES

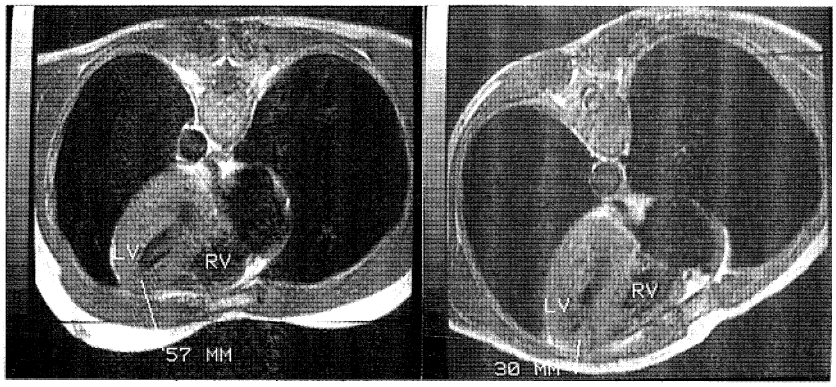

Figure 6. 2 min cardiac-gated ^{1}H NMR images recorded from the same normal subject (PAB) during the same imaging session in a supine (left) and a substantially prone (right) orientation showing the left (LF) and right (RV) ventricles of the heart. The prone orientation has reduced the LV distance from the surface from 57 mm to 30 mm (indicated), relative to the supine orientation.

skeletal and cardiac muscle, possess the same T_1 values (Bottomley *et al.* 1990*b*). The mean correction factor for saturation of the myocardial PCr/ATP ratio measured by this means was 1.38 ± 0.26 (SD) with the RF pulse power adjusted to maximize the PCr signal in unlocalized 6.5 cm surface coil spectra from the chests of 67 adults, recorded at a mean heart rate of 77.5 ± 14.7 min^{-1} ($T_R = 0.774 \pm 0.122$ s).

A similar method for correction can be applied to volume spectroscopic imaging of the brain: when sensitivity prohibits measurements of saturation factors on small voxels, choice of larger voxels may suffice. For example we have used whole section-averaged saturation corrections for brain ^{31}P spectroscopic imaging (Bottomley *et al.* 1988). Contribution from superficial muscle tissue are much less of a problem compared with the chest since the brain is the dominant metabolite source in axial sections (Bottomley & Hardy 1989).

It is arguable that reliable saturation corrections can be better made assuming T_1 measurements from a separate study of relaxation times usually performed on normal tissue. However, since $F = [1 - \exp(-T_R/T_1)] \sin\alpha$, the NMR flip angle, α, must still be reliably measured during each study with T_R varying, for example, due to different heart rates. Moreover, the T_1 values in the study group may differ from those in the T_1 control group due to disease, and T_1 measurements are notoriously error prone and hence unreliable. For example, normal brain PCr T_1 measurements from different laboratories vary from 3.1 to 5 s, and T_1 values can increase by 50% in brain tumours (Hubesch *et al.* 1990). It is not clear, therefore, whether this approach offers any advantage over direct measurements of saturation factors on each patient.

6. Exemplary applications

Metabolite ratios

Measurements of metabolite ratios abound in the *in vivo* ^{31}P NMR literature (Bottomley 1989; Radda *et al.* 1989) because they are easiest to make and all corrections for relaxation and localization artefacts may be ignored in individual studies where data are acquired under identical conditions. Unfortunately this usually means that results from different studies and laboratories are not

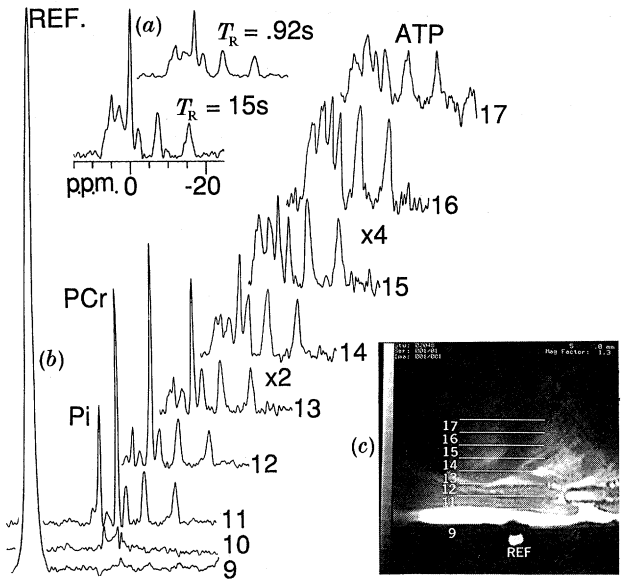

Figure 7. Data from a complete ^{31}P NMR exam of a normal heart. Volume-averaged spectra used for measuring saturation factors are shown in (*a*). (*b*) depicts a subset of 9 of 32 1D localized ^{31}P spectra from adjacent 1 cm thick slices through a phosphonitrilic chloride trimer reference (REF., slice 9), chest muscle (slices 11, 12) and the myocardium (slices 13–17). The corresponding ^{1}H surface coil image showing the location of the slices and the reference relative to the myocardium is displayed in (*c*).

Table 1. *Protocol for* ^{31}P *heart studies*

1. Position patient with chest on ^{31}P coil.
2. Establish cardiac gate.
3. Acquire ^{1}H image. Confirm coil location relative to heart.
4. Switch to spectroscopy.
5. Shim magnet on surface-coil ^{1}H spectrum.
6. Switch to ^{31}P. Adjust RF power to maximize PCr.
7. Acquire surface-coil spectra at heart rate and at T_R = 15 s.
8. Acquire localized ^{31}P spectra.

quantitatively comparable. The situation is significantly improved by minor protocol modifications such as the use of a uniform excitation field and by making volume-averaged saturation corrections as discussed above.

Table 1 summarizes a working protocol for ^{31}P studies of heart patients using the heart coil set (figure 3), and a 1D spatial encoding ^{31}P localization sequence with the encoding gradient directed along the axis of the receiving surface coil. Crude localization in the two dimensions orthogonal to the axis is afforded by the fade-off in the coils' sensitivity profile at the edges (Bottomley *et al.* 1985). An example of a complete data-set comprising a ^{1}H image, a set of localized ^{31}P spectra and unlocalized surface coil spectra for measuring saturation factors, is shown in figure 7. Note that the integrated (corrected) PCr/ATP ratio decreases from *ca.* 4 in the spectral slices that correspond to chest muscle to *ca.* 1.7 in the heart, consistent with earlier findings (Bottomley 1985; Blackledge *et al.* 1987). However, an observation of the decrease itself, in the absence of a corresponding image, is not an infallible

indicator of myocardial slices since in some patients, usually elderly women, the chest muscle contributions can be negligible and no clear transition is observed. Measurements of cardiac metabolite ratios may be of value in assessing metabolic changes in myocardial infarction (Bottomley *et al.* 1987), ischemia (Bottomley *et al.* 1989*c*) cardiomyopathy, left ventricular hypertrophy (Schaefer *et al.* 1990), and rejecting heart transplants (Herfkens *et al.* 1988).

Metabolite concentrations

If metabolite ratios are undisturbed and/or/but there is reason to believe that metabolite levels are altered, for example in stroke (Bottomley *et al.* 1986), tumours (Hubesch *et al.* 1990*b*), or dementia (Bottomley *et al.* 1990*a*), it may be desirable to attempt absolute quantitation. This is done by incorporating a reference of known concentration, $[r]$, within the range of the detection coil and comparing the integrated signals from the metabolite, S_p, and reference, S_r, in their respective voxels. Ideally the reference should fall outside the *in vivo* chemical shift range (Bottomley & Hardy 1989). The metabolite concentration estimates $[p]$, must be corrected for relaxation and field uniformity:

$$[p] = S_p[r]\, V_r \psi_r \Phi_r F_r E_r / \sigma S_r\, V_p \psi_p \Phi_p F_p E_p,$$

where σ, V, ψ and E are the tissue specific gravity, the volume of the sample in the voxel containing the reference (subscript r) and the metabolite (subscript p), the relative sensitivity of the detection coil at each voxel, and the attenuation factors for signal loss that occurs during T_d, respectively. A study protocol the same as in table 1 is suitable, except that values for all of the parameters must be obtained, and a full 3D-resolved localization sequence used. The percentage error in $[p]$ is the sum of those in all of the constituent parameters, so the likelihood of significant systematic error in the measurements is disturbingly high (Bottomley & Hardy 1989).

An example of metabolite concentration measurements in the human heart performed by this means appears elsewhere (Bottomley *et al.* 1990*b*): the myocardial volumes were measured from multislice ^{1}H NMR images and the spectra localized by slice-selective 3D spectroscopic imaging. Mean myocardial [PCr] was 11.0 ± 2.7 (SD) μmol (g wet mass)$^{-1}$ and [ATP] $= 6.9 \pm 1.6$ μmol g^{-1}.

Much of the concern about systematic errors in these measurements can be alleviated by eliminating the correction factors by designing experimental protocols that sacrifice spatial resolution for sensitivity per unit scan time. For example, by localizing only to a whole axial section in the brain using a slice-selective 180° pulse followed by a hard 90° NMR pulse sequence at $T_R = 15$ s, and by utilizing a uniform birdcage NMR coil (figures 3, 4), the ψ, Φ, F and E corrections can be omitted and the error effectively reduced to the random errors in the measured signals. Again, the brain tissue volume can be measured from a ^{1}H image of the same section. This approach is more appropriate for studying global disorders, or for calibrating concentrations in spectroscopic images acquired subsequently from the same sections at a finer spatial resolution. Indeed we have observed significant metabolic deficits in AIDS dementia using this technique (Bottomley *et al.* 1990*a*). In normal brain, the method yields [PCr] and [ATP] values of 4.92 ± 0.13 (SD) and 2.79 ± 0.11 μmol (g wet mass)$^{-1}$, respectively ($n = 29$).

7. Conclusions

In vivo ^{31}P NMR spectroscopy protocols are unlike those of its sister technology, ^{1}H NMR imaging, with its relatively lavish sensitivity, spatial resolution, and localization procedures restricted to one or two basic approaches that are largely independent of the disease under investigation. The poverty of ^{31}P NMR sensitivity to phosphate metabolites results in operating conditions that typically fall close to the bare minimum for useful detection. To maximize the value and reproducibility of the ^{31}P information, prudent but often painful choices between spatial resolution, localization technique, and distortions caused by NMR relaxation processes, are a necessity with this technology that must be faced at, or before, the time of the NMR exam. These choices will vary with the organ and disease to be studied, as well as with the nature of the information desired, whether metabolite ratios or concentrations. It is clearer than ever that spectroscopy requires versatility of techniques and instrumentation, both hardware and software, if it is to progress toward the ultimate goals of enhancing diagnostic and therapeutic medicine and contributing to the understanding of disease states.

References

Aue, W. P. 1986 Localization methods for *in vivo* nuclear magnetic resonance spectroscopy. *Rev. magn. Reson. Med.* **1**, 21–72.

Blackledge, M. J., Rajapopalan, B., Oberhaensli, R. D., Bolas, N. M., Styles, P. & Radda, G. K. 1987 Quantitative studies of human cardiac metabolism by P-31 rotating frame NMR. *Proc. natn. Acad. Sci. U.S.A.* **84**, 4283–4287.

Bottomley, P. A. 1985 Noninvasive study of high-energy phosphate metabolism in human heart by depth-resolved ^{31}P NMR spectroscopy. *Science, Wash.* **229**, 769–772.

Bottomley, P. A. 1989 Human *in vivo* NMR spectroscopy in diagnostic medicine: clinical tool or research probe? *Radiology* **170**, 1–15.

Bottomley, P. A., Charles, H. C., Roemer, P. B., Flamig, D., Engeseth, H., Edelstein, W. A. & Mueller, O. M. 1988 Human *in vivo* phosphate metabolite imaging with ^{31}P NMR. *Magn. reson. Med.* **7**, 319–336.

Bottomley, P. A., Drayer, B. D. & Smith, L. S. 1986 Chronic adult cerebral infarction studied by phosphorus NMR spectroscopy. *Radiology* **160**, 763–766.

Bottomley, P. A., Foster, T. H. & Darrow, R. D. 1984*a* Depth resolved surface coil spectroscopy for *in vivo* ^{1}H, ^{31}P, and ^{13}C NMR. *J. magn. Reson.* **59**, 338–342.

Bottomley, P. A. & Hardy, C. J. 1987 Progress in efficient three-dimensional spatially localized *in vivo* ^{31}P NMR spectroscopy using multidimensional spatially selective (ρ) pulses. *J. magn. Reson.* **74**, 550–556.

Bottomley, P. A. & Hardy, C. J. 1989 Rapid, reliable *in vivo* assays of human phosphate metabolites by nuclear magnetic resonance. *Clin. Chem.* **35**, 392–395.

Bottomley, P. A., Hardy, C. J., Cousins, J. P., Armstrong, M. & Wagle, W. A. 1990*a* AIDS dementia complex: brian high-energy phosphate metabolite deficits. *Radiol.* **176**, 407–411.

Bottomley, P. A., Hardy, C. J. & Roemer, P. B. 1990*b* Phosphate metabolite imaging and concentration measurements in human heart by nuclear magnetic resonance. *Magn. reson. Med.* **14**, 425–434.

Bottomley, P. A., Hardy, C. J., Roemer, P. B. & Mueller, O. M. 1989*a* Proton decoupled, Overhauser enhanced, spatially-localized carbon-13 spectroscopy in humans. *Magn. reson. Med.* **12**, 348–363.

Bottomley, P. A., Hardy, C. J., Roemer, P. B. & Weiss, R. G. 1989*b* Problems and expediencies in human ^{31}P spectroscopy. The definition of localized volumes, dealing with saturation and the technique-dependence of quantification. *NMR Biomed.* **2**, 284–289.

Bottomley, P. A., Hart, H. R., Edelstein, W. A., Schenck, J. F., Smith, L. S., Leue, W. M., Mueller, O. M. & Redington, R. W. 1984*b* Anatomy and metabolism of the normal human brain studied by magnetic resonance at 1.5 Tesla. *Radiology* **150**, 441–446.

Bottomley, P. A., Herfkens, R. J., Smith, L. S. & Bashore, T. M. 1987 Altered phosphate metabolism in myocardial infarction: P-31 NMR spectroscopy. *Radiology* **165**, 703–707.

Bottomley, P. A., Smith, L. S., Leue, W. M. & Charles, C. 1985 Slice-interleaved depth-resolved surface-coil spectroscopy (SLIT DRESS) for rapid ^{31}P NMR *in vivo*. *J. magn. Reson.* **64**, 347–351.

Bottomley, P. A., Weiss, R. G., Hardy, C. J., Schulman, S. P. & Gerstenblith, G. 1989*c* High energy phosphate metabolism in the heart monitored by ^{31}P NMR spectroscopy in patients with coronary artery disease. In *Book of abstracts, Society of Magnetic Resonance in Medicine 1989*, vol. 1, p. 35. Berkeley, California: Society of Magnetic Resonance in Medicine.

Buchthal, S. D., Thoma, W. J., Taylor, J. S., Nelson, S. J. & Brown, T. R. 1989 *In vivo* T_1 values of phosphorus metabolites in human liver and muscle determined at 1.5 T by chemical shift imaging. *NMR Biomed.* **2**, 198–304.

Brown, T. R., Kincaid, B. M. & Ugurbil, K. 1982 NMR chemical shift imaging in three dimensions. *Proc. natn. Acad. Sci. U.S.A.* **79**, 3523–3526.

Cady, E. B., de L. Costello, A. M., Dawson, M. J., Delpy, D. T., Hope, P. L., Reynolds, E. O. R., Tofts, P. S. & Wilkie, D. R. 1983 Noninvasive investigation of cerebral metabolism in newborn infants by phosphorus nuclear magnetic resonance spectroscopy. *Lancet* **i**, 1059–1063.

Conway, M. A., Briston, J. D., Blackledge, M. J. & Rajagopalan, B. 1988 Cardiac metabolism during exercise measured by magnetic resonance spectroscopy [letter]. *Lancet* **ii**, 692.

Coutts, G. A., Bryant, D. J., Collins, A. G., Cox, I. J., Sargentoni, J. & Gadian, D. G. 1989 ^{31}P magnetic resonance spectroscopy of the normal human brain: approaches using four dimension chemical shift imaging and phase mapping techniques. *NMR Biomed.* **1**, 190–197.

Edelstein, W. A., Glover, G. H., Hardy, C. J. & Redington, R. W. 1986 The intrinsic signal-to-noise ratio in NMR imaging. *Magn. reson. Med.* **3**, 604–618.

Edwards, R. H. T., Dawson, M. J., Wilkie, D. R., Gordon, R. E. & Shaw, D. 1982 Clinical use of nuclear magnetic resonance in the investigation of myopathy. *Lancet* **i**, 725–731.

Glover, G. H., Hayes, C. E., Pelc, N. J., Edelstein, W. A., Mueller, O. M., Hart, H. R.,Hardy, C. J., O'Donnell, M. & Barber, W. D. 1985 Comparison of linear and circular polarization for magnetic resonance imaging. *J. magn. Reson.* **64**, 255–270.

Hardy, C. J., Bottomley, P. A., Roemer, P. B. & Redington, R. W. 1988 Rapid ^{31}P spectroscopy on a 4-T whole-body system. *Magn. reson. Med.* **8**, 104–109.

Hayes, C. E., Edelstein, W. A., Schenck, J. F., Mueller, O. M. & Eash, M. 1985 An efficient highly homogeneous radio frequency coil for whole-body NMR imaging at 1.5 T. *J. magn. Reson.* **63**, 622–628.

Herfkens, R. J., Charles, H. C., Negro-Vilar, R., VanTrigt, P. 1988 *In vivo* phosphorus-31 NMR spectroscopy in human heart transplants. In *Book of abstracts, Society of Magnetic Resonance in Medicine 1988*, vol. 2, p. 827. Berkeley, California: Society of Magnetic Resonance in Medicine.

Hubesch, B., Sappey-Marinier, D., Roth, K., Meyerhoff, D. J., Matson, G. B. & Weiner, M. W. 1990 P-31 MR spectroscopy of normal human brain and brain tumors. *Radiology* **174**, 401–409.

Ordidge, R. J., Connelly, A. & Lohman, J. A. B. 1986 Image selection *in vivo* spectroscopy (ISIS). A new technique for spatially selective NMR spectroscopy. *J. magn. Reson.* **66**, 283–294.

Radda, G. K., Rajagopalan, B. & Taylor, D. J. 1989 Biochemistry *in vivo*: an appraisal of clinical magnetic resonance spectroscopy. *Magn. Reson. Q.* **5**, 122–151.

Ross, B. D., Radda, G. K., Gadian, D. G., Rocker, C. T., Esiri, M. & Falconer-Smith, J. 1981 Examination of a case of suspected McAdrle's syndrome by ^{31}P nuclear magnetic resonance. *N. Engl. J. Med.* **304**, 1338–1342.

Schaefer, S., Gober, J. R., Schwartz, G. G., Twieg, D. B., Weiner, M. W. & Massie, B. 1990 *In vivo* phosphorus-31 spectroscopic imaging in patients with global myocardial disease. *Am. J. Cardiol.* **65**, 1154–1161.

Tropp, J. S., Sugiura, S., Derby, K. A., Suzuki, Y., Hawryszko, C., Yamagata, H., Klein, J. E., Ortendahl, D. A., Kaufman, L. & Acosta, G. F. 1988 Characterization of MR spectroscopic imaging of the human head and limb at 2.0 T. *Radiology* **169**, 207–212.

PHILOSOPHICAL TRANSACTIONS OF THE ROYAL SOCIETY A MATHEMATICAL, PHYSICAL & ENGINEERING SCIENCES

Weiner, M. W., Hetherington, H., Hubesch, B., Karczmar, G., Massie, B., Maudsley, A., Meyerhoff, D. J., Sappey-Maninier, D., Schaefer, S., Twieg, D. & Matson, G. B. 1989 Clinical magnetic resonance spectroscopy of brain, heart, liver, kidney and cancer. A quantitative approach. *NMR Biomed.* **2**, 290–297.

Discussion

P. Mansfield (*University of Nottingham, U.K.*). It is understandable that the initial thrust of spectroscopic imaging should be directed to basic science studies of disease. Dr Bottomley indicated three main areas of application: namely basic science study of disease, monitoring of therapies including drugs and clinical use. Professor Radda is optimistic about the clinical use of ^{31}P for diagnosis of a number of genetic diseases. How does Dr Bottomley feel about clinical use in your applications?

P. A. Bottomley. Whether or not our studies will lead to true clinical applications in the day-to-day operation of a hospital scanner remains an open question. When promising experimental results are found from this or that particular study, they must first be reproduced at multiple sites on a much larger patient basis. If the results are positive, the efficacy of the application in terms of cost and value of the spectroscopic information relative to existing technologies must be evaluated, then ultimately a basis for reimbursement established. We are clearly a long way from this type of clinical application: as I have indicated, we must first deal with the reproducibility and comparability of data acquired in similar studies under similar and different protocols.

R. G. Shulman. I feel that too much emphasis has been placed upon a clinical use of spectroscopy of the sort that would require this to be a rather routine clinical measurement. In my opinion the main contributions of NMR spectroscopy to medicine will be in the elucidation of mechanisms and basic biochemical understanding. In this direction we have almost unlimited exciting prospects for understanding which should provide a stronger basis for medical treatment.

D. Menon (*Hammersmith Hospital, London, U.K.*). (1) Dr Bottomley has made a point that spatial localization can be sacrificed when a disease uniformly involves a whole organ. Is not the assessment of cardiac transplant rejection an ideal scenario to apply this practice? (2) Could the advantages of the prone position be duplicated by applying the surface coil firmly to the chest of a supine position?

P. A. Bottomley. (1) Yes. The question is: what localization technique is best suited to acquiring a spectrum from the entire heart? When we started the study probably only the 'ISIS' technique could be applied in this manner. However, ISIS is a difference technique and we were very concerned about localization errors resulting from physiological motions. We therefore used the phase-encoding approach. It is possible that a simple surface-spoiling approach could be used for transplant studies, with surface-coil detection. (2) The supine orientation has the additional problem that the surface coil on the chest will move up and down with breathing (see text).

PHILOSOPHICAL TRANSACTIONS OF THE ROYAL SOCIETY A MATHEMATICAL, PHYSICAL & ENGINEERING SCIENCES

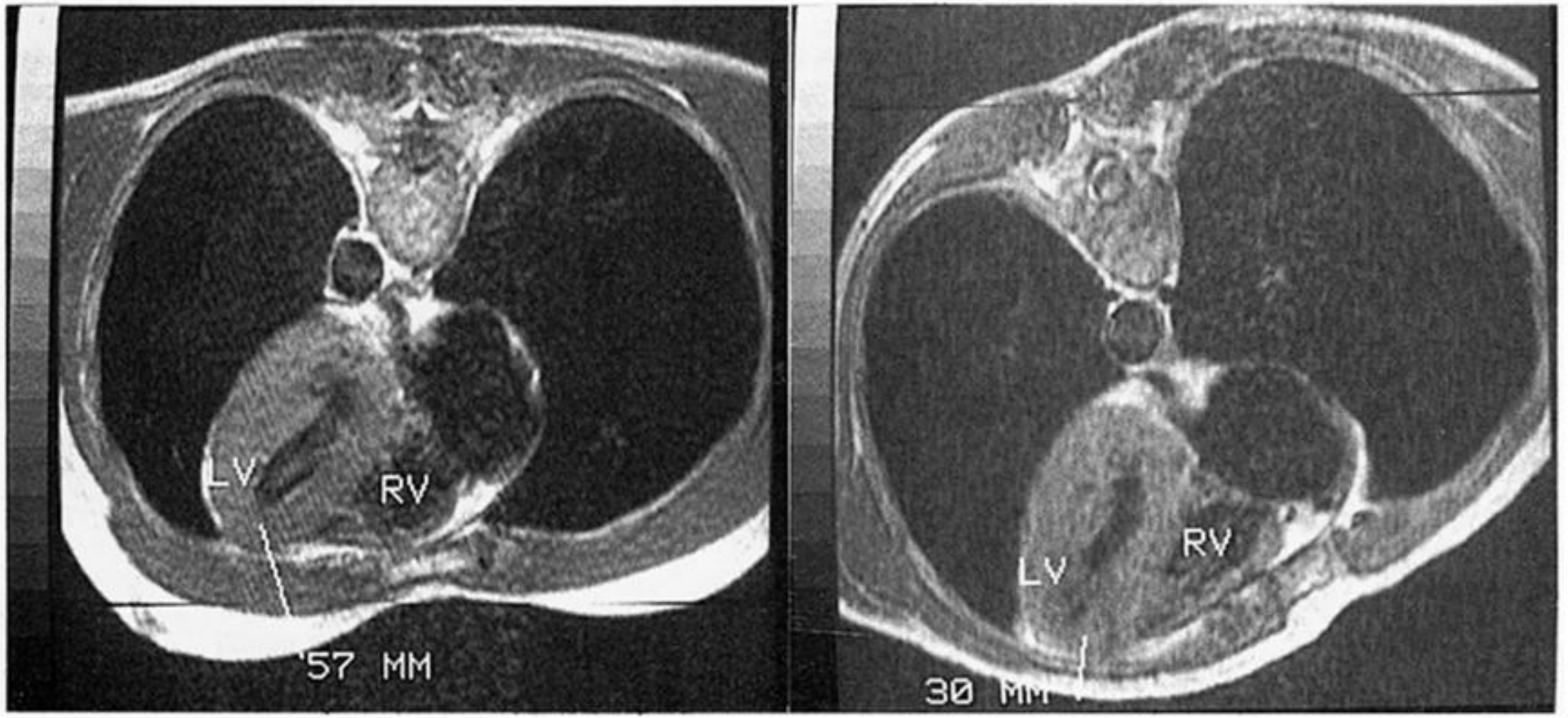

gure 6. 2 min cardiac-gated ^{1}H NMR images recorded from the same normal subject (PAB) during e same imaging session in a supine (left) and a substantially prone (right) orientation showing the ft (LF) and right (RV) ventricles of the heart. The prone orientation has reduced the LV distance om the surface from 57 mm to 30 mm (indicated), relative to the supine orientation.

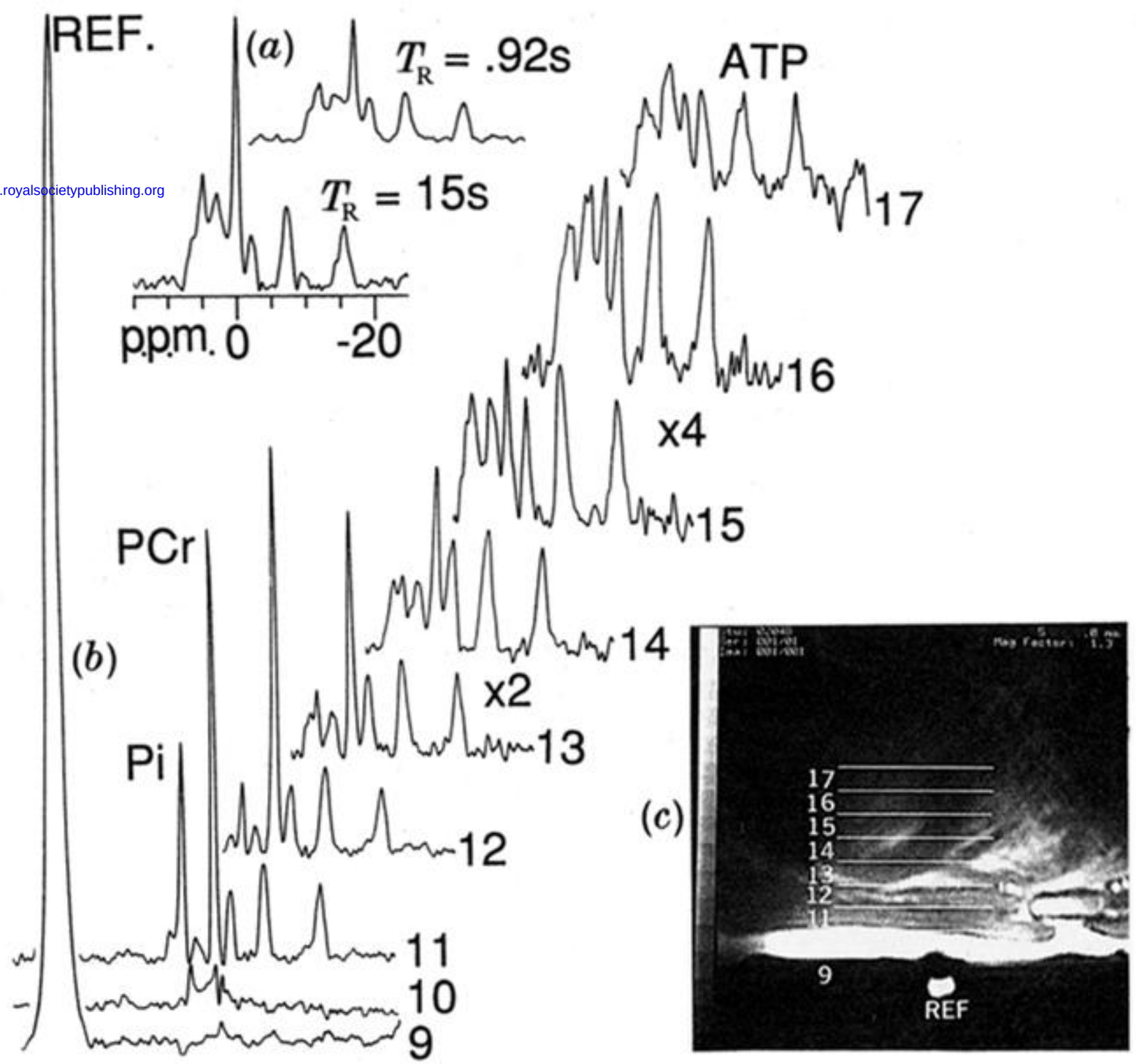

gure 7. Data from a complete ^{31}P NMR exam of a normal heart. Volume-averaged spectra used r measuring saturation factors are shown in (*a*). (*b*) depicts a subset of 9 of 32 1D localized ^{31}P ectra from adjacent 1 cm thick slices through a phosphonitrilic chloride trimer reference (REF., ce 9), chest muscle (slices 11, 12) and the myocardium (slices 13–17). The corresponding ^{1}H rface coil image showing the location of the slices and the reference relative to the myocardium displayed in (*c*).